Assessment of the Titanium Dioxide Absorption Coefficient by Grazing-Angle Fourier Transform Infrared and Ellipsometric Measurements

FABIO VARIOLA, ANTONIO NANCI, and FEDERICO ROSEI*

INRS-EMT, Université du Québec, 1650 Boul. Lionel-Boulet, Varennes, QC, J3X 1S2, Canada (F.V., F.R.); and Laboratory for the Study of Calcified Tissues and Biomaterials, Faculté de Médecine Dentaire, Université de Montréal, Montreal, QC, H3C 3J7, Canada (F.V., A.N.)

Index Headings: **Ellipsometry; Infrared spectroscopy; IR spectroscopy; Thin solid films; Biomaterials; Nanostructured materials; Grazing-angle Fourier transform infrared spectroscopy.**

INTRODUCTION

Thin films, either deposited or native (i.e., oxide layers), have been widely exploited in different technological fields (e.g., optics, electronics, and biomedicine) to improve the efficiency of devices and extend their range of applications. Among the different physical/chemical characteristics of thin layers that determine their overall properties and therefore their potential for new applications, thickness has been demonstrated to play a pivotal role in affecting different phenomena; this is particularly significant at nanoscale dimensions, since nanostructured materials often behave very differently from their bulk counterparts.[1] For example, thickness affects the microstructure, morphology, and optoelectronic properties of ZnS,[2] ZnO,[3,4] and Mo-doped indium oxide[4] thin films, as well as the electrical properties of MOS structures[5] in microelectronic and optical devices. In the biomedical field, the thickness of the superficial TiO_2 layer affects the biological response of titanium-based materials.[6–8]

Due to its effects on several optical, physical, and biological events, different techniques have been developed to precisely determine the thickness of thin oxide layers, such as, for example, that of SiO_2[9] and TiO_2.[10] However, the majority of these methods have limitations[9] that can compromise their applicability to a wide range of samples and materials. In addition, these techniques (e.g., X-ray photoelectron spectroscopy (XPS) sputter profiling[9]) may damage the sample surface and alter its micro and nanometric topographical features. One of the most efficient nondestructive methods to precisely measure the thickness of thin organic and inorganic layers is ellipsometry.[11–16]

Infrared (IR) spectroscopy has found increasing applications in materials science, biology, and nanotechnology due to the possibility of determining the surface chemical composition of thin inorganic[17–20] and molecular layers.[21–27] However, to our knowledge, this technique has never been used to determine quantitatively the thickness of inorganic thin films.

In this work, we demonstrate that ellipsometry and Fourier transform infrared (FT-IR) spectroscopy can be combined to estimate the absorption coefficient and the thickness of IR-active nanometric oxide layers. In particular, we selected the amorphous TiO_2 layer present on the surfaces of bulk titanium (cpTi) and Ti6Al4V resulting from natural passivation and chemical oxidation with H_2SO_4/H_2O_2 solutions.[28–33] Results from this study will permit the exclusive use of FT-IR to determine the thickness of amorphous titanium dioxide thin films. More generally, our approach can be potentially applied to investigate a wider variety of materials (IR-active thin films deposited on a reflective substrate), without altering their surface topography.

EXPERIMENTAL

The creation of different TiO_2 layers on titanium (cpTi) and Ti6Al4V by controlled chemical oxidation with 36 N H_2SO_4 and 30% aqueous H_2O_2 solutions has been detailed elsewhere.[28–33] In these studies, it was demonstrated that the chemical treatment mainly modifies the topography and the thickness of the protective TiO_2 layer, by introducing submicrometer and nanoscale textures. Raman and XPS spectroscopy measurements demonstrated that its chemical composition and amorphous nature were not significantly affected.[30,31]

In the present study, IR spectroscopy was used to probe native and modified oxide layers. A Nexus 870 FT-IR spectrometer equipped with a SAGA (smart aperture grazing angle) accessory (Thermo Nicolet, Madison, WI) was used. The analysis of the thin oxide layer was performed in grazing-angle mode at an angle of 80° with respect to the surface normal, using a spectral resolution of 4 cm^{-1} in the 475–1100 cm^{-1} range. Spectroscopic information was collected from an 8 mm diameter area. A gold substrate was used to collect a background spectrum for reference. Spectra were finally fitted by PeakFit software (Systat Software, San Jose, CA) using Gaussian–Lorentzian functions and a linear baseline (Fig. 1). Three Gaussian–Lorentzian curves were used to fit the absorption band in the 475–1050 cm^{-1} range, centered at 610 ± 2 cm^{-1}, 820 ± 2 cm^{-1}, 895 ± 5 cm^{-1} (Control cpTi), 650 ± 10 cm^{-1}, 830 ± 10 cm^{-1}, 920 ± 5 cm^{-1} (Treated cpTi), 610 ± 1 cm^{-1}, 845 ± 5 cm^{-1}, and 925 ± 10 cm^{-1} (control Ti6Al4V) and 660 ± 20 cm^{-1}, 825 ± 15 cm^{-1}, and 920 ± 10 cm^{-1} (treated Ti6Al4V), respectively. The band located near 600 cm^{-1} can be assigned to Ti–O stretching vibrations for Ti atoms in octahedral surroundings,[34,35]

Received 12 May 2009; accepted 16 July 2009.
* Author to whom correspondence should be sent. E-mail: rosei@emt.inrs.ca.

0003-7028/09/6310-1187$2.00/0

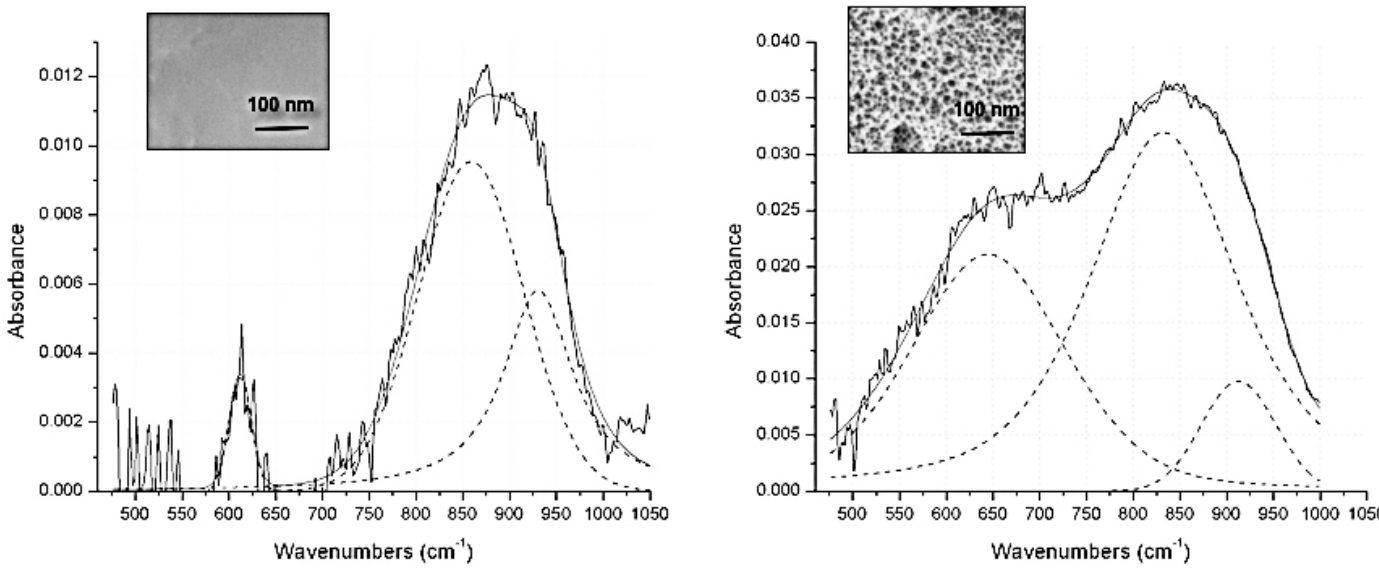

FIG. 1. Grazing-angle FT-IR spectra of (**left**) control and (**right**) treated (3:1 v/v H_2SO_4/H_2O_2 at 50 °C) titanium. The Gaussian–Lorentzian curves used to fit the FT-IR spectra are also displayed (dashed lines).

whereas bands at about 800 cm^{-1} and 920 cm^{-1} are associated with atomic stretching vibration in a tetrahedral environment.[17]

The thickness of the oxide layer was estimated from optical measurements using a variable-angle spectroscopic VASE ellipsometer (J.A. Woollam Co., Lincoln, NE) and a double-beam Lambda 19 spectrophotometer (Perkin Elmer, Waltham, MA) in the wavelength range 300–900 nm. Ellipsometric measurements were evaluated at two different incidence angles (45° and 75°) with a 9.3 nm wavelength step. The experimental data were fitted by using the Bruggeman equation for composite materials.[36] In the case of treated samples, the graded layer was modeled as titanium metallic substrate plus a second composite material made of a mixture of TiO_2 and voids. For controls and untreated samples, a two-layer model (i.e., titanium metal plus titanium dioxide) was adopted. In all cases, the layer corresponding to the metallic substrate was modeled with Drude (absorption in the IR) and Lorentz (absorption in the ultraviolet–visible (UV-VIS) range) oscillators.

In previous work,[29,30] we demonstrated qualitatively the relation between the total integral area of the absorption peaks

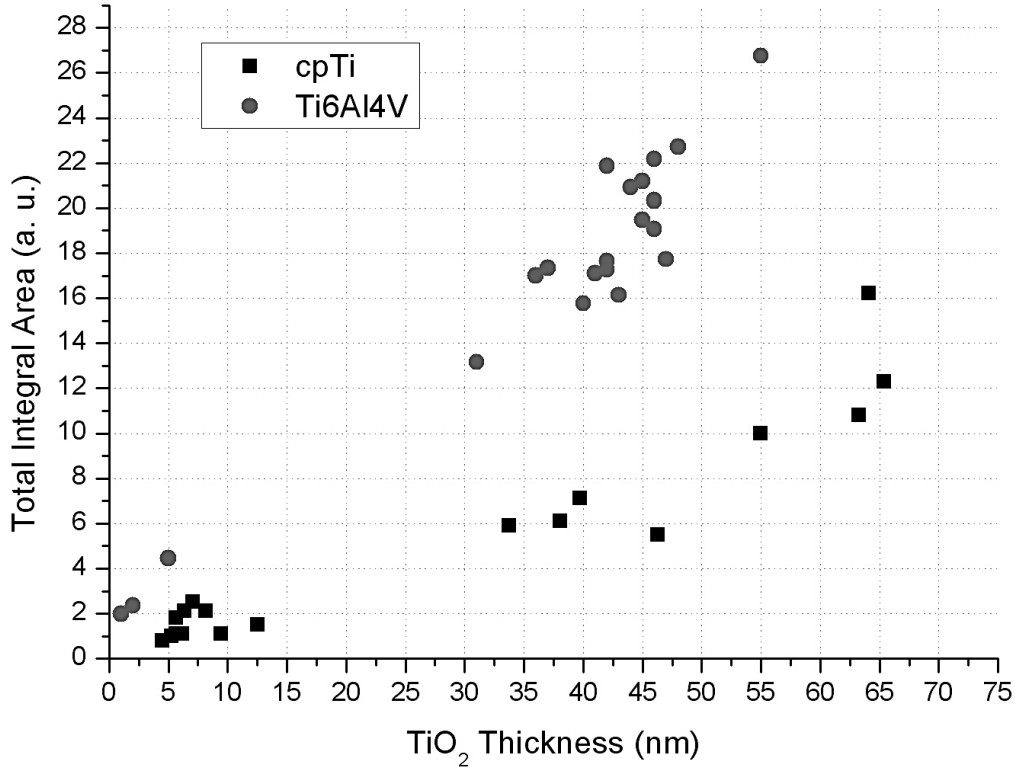

FIG. 2. Integrated Ti–O absorbance (FT-IR) versus TiO_2 thickness measured by ellipsometry, in the case of cpTi[28] (squares) and Ti6Al4V[29] (circles).

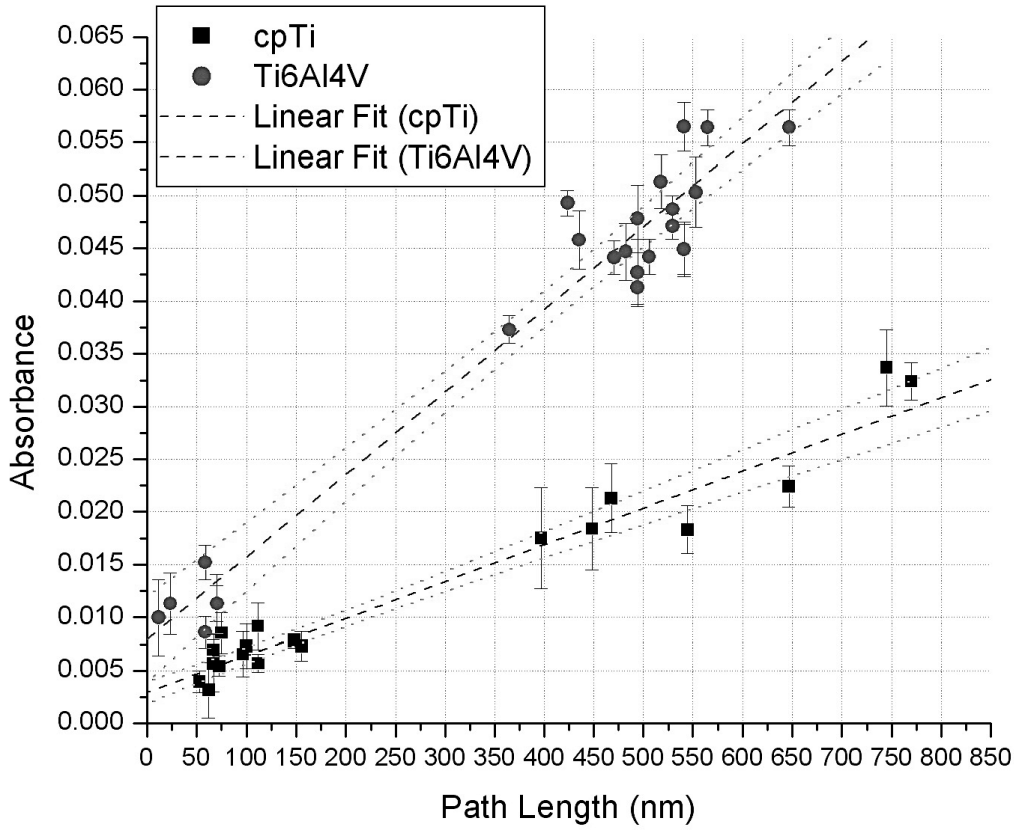

FIG. 3. Absorbance at 820 ± 2 cm^{-1} (Control cpTi), 830 ± 10 cm^{-1} (Treated cpTi), 845 ± 5 cm^{-1} (Control Ti6Al4V), and 825 ± 15 cm^{-1} (Treated Ti6Al4V) versus optical path calculated from ellipsometric results. Linear fit with 95% confidence bands are also plotted.

related to the Ti–O bonds in the 400–1000 cm^{-1} range and the thickness of the TiO_2 layer estimated by ellipsometry. Figure 2 illustrates quantitatively this relation in the case of pristine and modified oxide layers on cpTi and Ti6Al4V. The correlation between the IR absorption peak in the 400–1000 cm^{-1} region and TiO_2 thickness has also been qualitatively demonstrated in theoretical simulations by Transferetti et al.[37]

In general, the correlation between the intensity of the IR absorption peak and the thickness of the probed material is linear and described by the Lambert–Beer law ($A = \alpha l$ where A is the absorbance, α is the absorption coefficient, and l is the path length of light throughout the material). To verify whether our experimental results follow this relation, we plotted (Fig. 3) the absorbance of the band located in the 800–900 cm^{-1} region (i.e., the band with the greater intensity compared to the other two) with the path length of the IR beam throughout the sample calculated by simple geometrical considerations. The linearity was determined by carrying out a linear fit of raw data (dotted lines in Fig. 3) using Origin software (OriginLab Corporation, Northampton, MA). The resulting analytical expressions of the linear relations in the case of cpTi and Ti6Al4V are, respectively,

$$y_{\mathrm{cpTi}} = (2.78 \pm 0.86) \times 10^{-3} + (3.63 \pm 0.22) \times 10^{-5} x \quad (R^2 = 0.95)$$

and

$$y_{\mathrm{Ti6Al4V}} = (6.14 \pm 2.29) \times 10^{-3} + (8.11 \pm 0.49) \times 10^{-5} x \quad (R^2 = 0.93)$$

From Figure 3 and from the equations above, we infer that the linear function intercepts the y-axis (i.e., absorbance) at values very close to zero when x (i.e., path length) is zero, thus providing additional evidence that data follow the linear Lambert–Beer law. According to this principle, we can extrapolate the absorption coefficient from the slope of the two lines, thus $\alpha_{\mathrm{cpTi}} = 363 \pm 22$ cm^{-1} and $\alpha_{\mathrm{Ti6Al4V}} = 811 \pm 49$ cm^{-1} for the amorphous titanium dioxide present on cpTi and Ti6Al4V, respectively. The different values in the absorption coefficient of TiO_2 growth on titanium and on the alloy may depend on the diverse composition of the oxide layer, which in the case of Ti6Al4V also includes Al_2O_3 and V_2O_5.[30]

CONCLUSION

Different thicknesses of the TiO_2 layer were generated by controlled chemical oxidation with H_2SO_4/H_2O_2 solutions. Although this method creates a network of nanometric pits, it preserves the natural physical and chemical characteristics of the native oxide. In fact, we have demonstrated that TiO_2 chemical composition and amorphous structure did not vary significantly.[30,31] Therefore, we can also assume that the oxide density was not modified by such a treatment. With respect to superficial morphology, the chemically generated nanoporosity was taken into account to create the mathematical model used to fit the ellipsometric results. This means that the calculated thicknesses were not affected by the topography. However, in the case of the alloy, the submicrometric cavities may have influenced the measurements (in the case of cpTi, only flat samples at micro- and macroscale were considered for the

present study). Nevertheless, the measured value of the absorption coefficient approximates well that of the protective TiO_2 layer resulting from the oxidation (natural and chemical) of cpTi and Ti6Al4V used in our studies.

Consequently, the determination of the absorption coefficient will now allow the thickness of amorphous titanium oxide to be estimated exclusively by FT-IR measurements. This approach can be thus applied to substrates that are not suitable for ellipsometry (e.g., microtextured titanium) as well as to nanostructured TiO_2 surfaces (e.g., nanotubular structures generated by anodization of titanium),[38,39] without alteration of their topographical features.

ACKNOWLEDGMENTS

We thank Prof. C. Reber and Dr. J. MacLeod for a critical reading of the manuscript. We also thank R. Vernhes for help in obtaining ellipsometric measurements. F.V. is grateful to A. Lauria and A. Bernardi for helpful discussions. We acknowledge funding from the Canadian Institutes of Health Research (CIHR) and the Natural Sciences and Engineering Research Council of Canada (NSERC) through a Collaborative Health Research Project grant. We thank NSERC for a Collaborative Research and Development grant with Plasmionique, Inc. (Varennes, QC, Canada). F.V. acknowledges the Canadian Bureau for International Education (CBIE) and FQRNT for financial support through personal fellowships. A.N. acknowledges funding from the CIHR and the Canada Foundation for Innovation. F.R. is grateful to the Fonds québécois de la recherche sur la nature et les technologies (FQRNT) and for start-up funds from INRS. F.R. also acknowledges support from the Canada Research Chairs Program and from NSERC (Discovery Grants).

1. F. Rosei, J. Phys. Condens. Matter **16,** S1373 (2004).
2. P. Prathap, N. Revathi, Y. P. V. Subbaiah, and K. T. R. Reddy, J. Phys. Condens. Matter **20,** 035205 (2008).
3. J. H. Chung, J. Y. Lee, H. S. Kim, N. W. Jang, and J. H. Kim, Thin Solid Films **516,** 5597 (2008).
4. T. P. Rao and M. C. Santhoshkumar, Appl. Surf. Sci. **255,** 4579 (2009).
5. R. K. Gupta, K. Ghosh, R. Patel, and P. K. Kahol, Appl. Surf. Sci. **255,** 3046 (2008).
6. N. Tugluoglu, S. Karadeniz, A. B. Selcuk, and S. B. Ocak, Physica B **400,** 168 (2007).
7. C. Eriksson, J. Lausmaa, and H. Nygren, Biomaterials **22,** 1987 (2001).
8. S. Kanagaraja, A. Wennerberg, C. Eriksson, and H. Nygren, Biomaterials **22,** 1809 (2001).
9. V. Muhonen, R. Heikkinen, A. Danilov, T. Jamsa, and J. Tuukkanen, J. Mater. Sci.: Mater. Med. **18,** 959 (2007).
10. D. A. Cole, J. R. Shallenberger, S. W. Novak, R. L. Moore, M. J. Edgell, S. P. Smith, C. J. Hitzman, J. F. Kirchhoff, E. Principe, W. Nieeven, F. K. Huang, S. Biswas, R. J. Bleiler, and K. Jones, J. Vac. Sci. Technol. B **18,** 440 (2000).
11. E. McCafferty and J. P. Wightman, Appl. Surf. Sci. **143,** 92 (1999).
12. D. Barriet, C. M. Yam, O. E. Shmakova, A. C. Jamison, and T. R. Lee, Langmuir **23,** 8866 (2007).
13. M. Gnauck, E. Jaehne, T. Blaettler, S. Tosatti, M. Textor, and H.-J. P. Adler, Langmuir **23,** 377 (2007).
14. R. D. Weinstein, J. Richards, S. D. Thai, D. M. Omiatek, C. A. Bessel, C. J. Faulkner, S. Othman, and G. K. Jennings, Langmuir **23,** 2887 (2007).
15. H. Elwing, Biomaterials **19,** 397 (1998).
16. K. Rechendorff, M. B. Hovgaard, M. Foss, V. P. Zhdanov, and F. Besenbacher, Langmuir **22,** 10885 (2006).
17. D. Velten, V. Biehl, F. Aubertin, B. Valeske, W. Possart, and J. Breme, J. Biomed. Mater. Res. **59,** 18 (2002).
18. A. Balamurugan, A. H. S. Rebelo, S. Kannan, J. M. F. Ferreira, J. Michel, G. Balossier, and S. Rajeswari, J. Biomed. Mater. Res. B **81,** 441 (2007).
19. F. Balas, T. Kokubo, M. Kawashita, and T. Nakamura, J. Mater. Sci.: Mater. Med. **18,** 1167 (2007).
20. S. Foppiano, S. J. Marshall, E. Saiz, A. P. Tomsia, and G. W. Marshall, Acta Biomater. **2,** 133 (2006).
21. V. Nelea, C. Morosanu, M. Bercu, and I. N. Mihailescu, J. Mater. Sci.: Mater. Med. **18,** 2347 (2007).
22. N. Adden, L. J. Gamble, D. G. Castner, A. Hoffmann, G. Gross, and H. Menzel, Biomacromol. **7,** 2552 (2006).
23. R. Aroca and D. J. Ross, Appl. Spectrosc. **58,** 324 (2004).
24. J. J. J. P. van den Beucken, M. R. J. Vos, P. C. Thune, T. Hayakawa, T. Fukushima, Y. Okahata, X. F. Walboomers, N. A. J. M. Sommerdijk, R. J. M. Nolte, and J. A. Jansen, Biomaterials **27,** 691 (2006).
25. T. Nagayasu, K. Imamura, and K. Nakanishi, J. Colloid Interface Sci. **286,** 462 (2005).
26. A. Raman, M. Dubey, I. Gouzman, and E. S. Gawalt, Langmuir **22,** 6469 (2006).
27. D. A. Trubitsyn and A. V. Vorontsov, J. Phys. Chem. B **109,** 21884 (2005).
28. A. Nanci, J. D. Wuest, L. Peru, P. Brunet, V. Sharma, S. F. Zalzal, and M. D. McKee, J. Biomed. Mater. Res. **40,** 324 (1998).
29. F. Variola, A. Lauria, A. Nanci, and F. Rosei, paper in preparation (2009).
30. F. Variola, J.-H. Yi, L. Richert, J. D. Wuest, F. Rosei, and A. Nanci, Biomaterials **29,** 1285 (2008).
31. J.-H. Yi, C. Bernard, F. Variola, S. F. Zalzal, J. D. Wuest, F. Rosei, and A. Nanci, Surf. Sci. **600,** 4613 (2006).
32. L. Richert, F. Vetrone, J.-H. Yi, S. F. Zalzal, J. D. Wuest, F. Rosei, and A. Nanci, Adv. Mater. **20,** 1488 (2008).
33. F. Vetrone, F. Variola, P. Tambasco de Oliveira, S. F. Zalzal, J.-H. Yi, J. Sam, K. F. Bombonato-Prado, A. Sarkissian, D. F. Perepichka, J. D. Wuest, F. Rosei, and A. Nanci, Nano. Lett. **9,** 659 (2009).
34. S. Amor, L. Guedri, G. Baud, M. Jacquet, and M. Ghedira, Mater. Chem. Phys. **77,** 903 (2002).
35. R. Urlaub, U. Posset, and R. Thull, J. Non-Cryst. Solids **265,** 276 (2000).
36. R. Vernhes, A. Amassian, J. Klemberg-Sapieha, and L. Martinu, J. Appl. Phys. **99,** 114315 (2006).
37. B. Trasferetti, C. Davanzo, R. Zoppi, N. Cruz, and M. Moraes, Phys. Rev. B **64,** 125404 (2001).
38. G. Balasundaram, C. Yao, and T. J. Webster, J. Biomed. Mater. Res. A **84,** 447 (2008).
39. C. Yao, E. B. Slamovich, and T. J. Webster, J. Biomed. Mater. Res. A **85,** 157 (2008).

Transfer of Calibrations for Barley Quality from Dispersive Instrument to Fourier Transform Near-Infrared Instrument

MIRYEONG SOHN,* DAVID S. HIMMELSBACH, FRANKLIN E. BARTON, II, and JAMES A. DE HASETH

Richard B. Russell Agricultural Research Center, ARS, USDA, P.O. Box 5677, Athens, Georgia 30605 (M.S., D.S.H., F.E.B.); Current address: University of Georgia, Department of Chemistry, Athens, Georgia 30605 (M.S., J.A.d.H.); Current address: Light Light Solutions, LLC, P.O. Box 81486, Athens, Georgia 30608-1486 (D.S.H., F.E.B.)

Index Headings: **Calibration transfer; Transfer samples; Near-infrared spectroscopy; NIR spectroscopy; Fourier transform near-infrared spectroscopy; FT-NIR spectroscopy; Barley; Starch; Protein.**

INTRODUCTION

In our previous studies,[1,2] we developed near-infrared (NIR) calibration models for quality assessment of barley as a source of fuel ethanol production. Both the dispersive system and

Received 12 May 2009; accepted 16 July 2009.

* Author to whom correspondence should be sent. E-mail: miryeong.sohn@ars.usda.gov.